Thermal Buckling Analysis of Laminated Composite Plates using Isogeometric Analysis [1-24]

Presented in honor of Prof. Romesh C. Batra's 70th Birthday

Balakrishnan Devarajan

Virginia Polytechnic Institute and State University
Blacksburg, Virginia 24060
USA

Outline

- Isogeometric Analysis
- Bezier Extraction : Motivation
- Bezier Extraction : Theory
- Plate Problem
- Numerical Investigation
- Analysis Procedure
- Results

Isogeometric Analysis

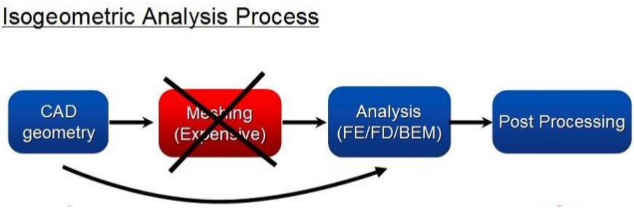

- Unifies the computer aided design (CAD) and the computer aided engineering (CAE) [1].
- Significant decrease in computational cost as the meshes are generated within the CAD.
- Higher accuracy results because of the smoothness and the higher order continuity between elements

1. Cottrell, J. Austin, Thomas JR Hughes, and Yuri Bazilevs. Isogeometric analysis toward integration of CAD and FEA. John Wiley Sons, 2009.

B-spline basis functions are expressed by a set of non-decreasing values called the knot vector

$$\Xi = \{\xi_1, \xi_2, \ldots, \xi_{n+p+1}\} \tag{1}$$

B-spline basis functions are defined by the following recursive form

$$N_{i,0}(\xi) = \begin{cases} 1 & \text{if } \xi_i \leq \xi < \xi_{i+1}, \\ 0 & \text{otherwise}, \end{cases} \quad \textit{for } p = 0 \tag{2}$$

$$N_{i,p}(\xi) = \frac{\xi - \xi_i}{\xi_{i+p} - \xi_i} N_{i,p-1}(\xi) + \frac{\xi_{i+p+1} - \xi}{\xi_{i+p+1} - \xi_{i+1}} N_{i+1,p-1}(\xi) \quad \text{for } p \geq 1 \tag{3}$$

where ξ_1 is the ith knot, n is the number of basis functions and p is the polynomial order.

Bezier Extraction : A Primer

- IGA is implemented with the presence of C^0 continuous Bézier elements
- The Bezier extraction operator decomposes the Non Uniform Rational B-Splines(NURBS) into C^0-continuous Bezier elements using linear combinations of Bernstein polynomials
- Bezier elements bear a close resemblance to the Lagrange elements used in finite element methods
- Allows easy incorporation into existing finite element codes without adding many changes as IGA

Bezier Extraction : Theory

Bézier decomposition[2] is accomplished by the insertion of new knots into the B-spline curve until k = p. Where k is the multiplicity of the knot

$$\bar{P}_i = \begin{cases} P_1 & i = 1 \\ a_i P_i + (1 - a_i) P_{i-1} & 1 < i < n+1 \\ P_n & i = n+1 \end{cases}, \tag{4}$$

$$a_i = \begin{cases} 1 & 1 \le i \le k - p \\ \frac{\bar{\xi} - \xi_i}{\xi_{i+1} - \xi_i} & k - p + 1 \le i \le k \\ 0 & i \ge k + 1 \end{cases}, \tag{5}$$

The new control points are expressed in matrix form as,

$$\mathbf{P}^{\mathrm{b}} = \mathbf{C}^T \mathbf{P} \tag{6}$$

---

2. Borden, Michael J., Michael A. Scott, John A. Evans, and Thomas JR Hughes. "Isogeometric finite element data structures based on Bézier extraction of NURBS." International Journal for Numerical Methods in Engineering 87, no. 1-5 (2011) : 15-47.

Knot Insertion : Visual Description

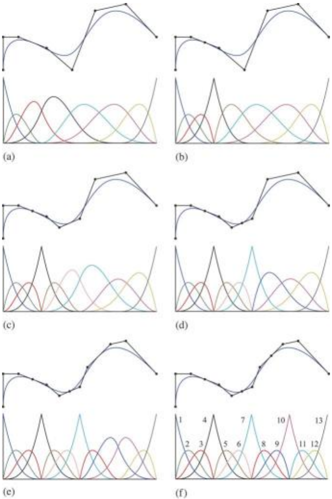

Bezier Extraction : Theory

The 2D NURBS basis functions which are written as

$$R_{i,j}(\xi,\eta) = \frac{N_{i,p}(\xi)M_{j,q}(\eta)w_{i,j}}{\sum_{i=1}^{n}\sum_{j=1}^{m} N_{i,p}(\xi)M_{j,q}(\eta)w_{i,j}}. \tag{7}$$

are now written in terms of Bernstein polynomials as

$$\mathbf{R}(\xi,\eta) = \frac{1}{W(\xi,\eta)}\mathbf{WN}(\xi,\eta) = \frac{1}{W(\xi,\eta)}\mathbf{WCB}(\xi,\eta), \tag{8}$$

The new control points are expressed as,

$$\mathbf{P}^{b} = (\mathbf{W}^{\mathrm{b}})^{-1}\mathbf{C}^{T}\,\mathbf{WP}, \tag{9}$$

Where $\mathbf{W}^{\mathbf{b}}$ and $\mathbf{W}$ are derived from the weights of the control points

Geometry : Construction and Mesh

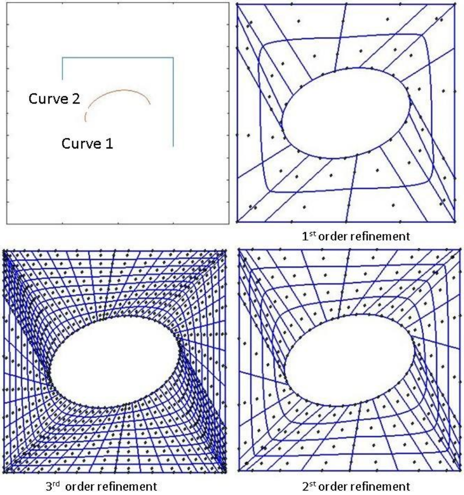

Plate Problem

Three-dimensional displacement field (u, v, w) of a four-layered unit square are expressed in terms of five unknown variables as :

$$u(x,y,z) = u_0(x,y) + z\varphi_x(x,y)$$
$$v(x,y,z) = v_0(x,y) + z\varphi_y(x,y)$$
$$w(x,y,z) = w_0(x,y)$$

where , $\frac{-h}{2} \leq z \leq \frac{h}{2}$

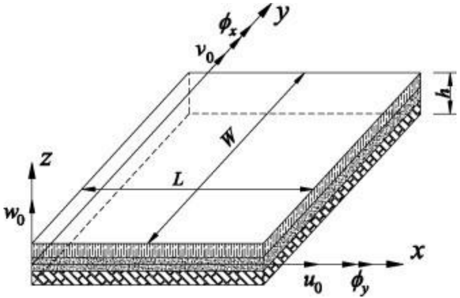

Numerical Investigation

- Material Property

$$E_L/E_T = 15,\ G_{LT}/E_T = 0.5,\ G_{TT}/E_T = 0.3356,\\ \nu_{LT} = 0.3,\ \nu_{TT} = 0.49,\ \alpha_L/\alpha_0 = 0.015,\ \alpha_T/\alpha_0 = 1 \tag{10}$$

- Boundary Condition

$$\textit{Clamped}:\quad \begin{array}{l} u_0 = v_0 = w_0 = \varphi_y = \varphi_x = 0 \quad \text{on } x = 0, L \\ u_0 = v_0 = w_0 = \varphi_x = \varphi_y = 0 \quad \text{on } y = 0, W \end{array} \tag{11}$$

- Loads : A unit temperature rise of 1 unit is applied on all the control points.

Analysis Procedure

- For the symmetric laminated plate subjected to a uniform temperature rise, only membrane forces are generated
- ABD matrix is calculated using the material properties
- A linear static analysis is then solved to determine the thermal in-plane resultants
- The stress resultants are then used to compute the initial stress stiffness matrix
- The stiffness matrix and the geometric stiffness matrix are used to solve the eigenvalue problem

Results

The critical buckling temperature is normalized as $\overline{T}_{cr} = \alpha_0 T_{cr}$

L/h	FSDT [3]	HSDT [3]	Present
100	0.3348	0.3352	0.3349
10	0.1655	0.1601	0.1656

Table – critical buckling temperature of a symmetric four-layer [0/90/90/0] laminated plate.10x10 mesh and $p = 2$

.

Thermal buckling mode shapes for various L/h ratios are presented.

3. Kant, T., and C. S. Babu. "Thermal buckling analysis of skew fibre-reinforced composite and sandwich plates using shear deformable finite element models." Composite Structures 49, no. 77 (2000) : 85.

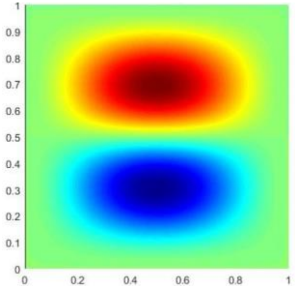

Figure – L/h= 100 (Present)

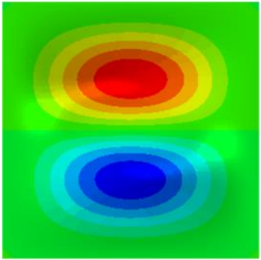

Figure – L/h= 100 (ABAQUS)

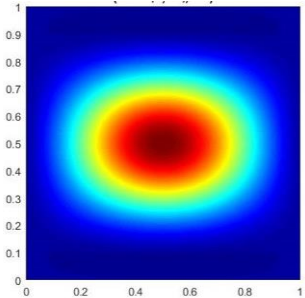

Figure – L/h= 10 (Present)

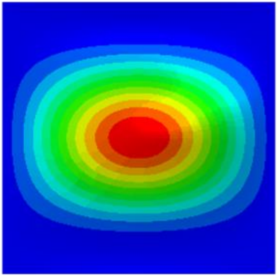

Figure – L/h= 10 (ABAQUS)

Plate with a Central Circular Cutout

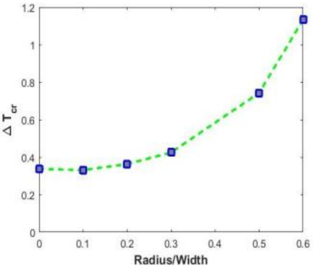

Figure – [0°/90°/90°/0°]

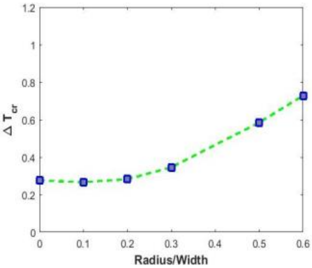

Figure – [45°/-45°/-45°/45°]

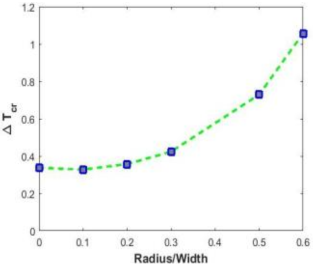

Figure – [90°/0°/0°/90°]

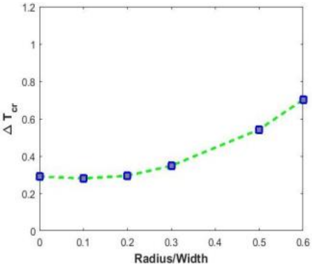

Figure – [60°/-60°/-60°/60°]

Numerical Investigation : Hybrid Composites

- Material Property - I

$$E_L/E_T = 15,\ G_{LT}/E_T = 0.5,\ G_{TT}/E_T = 0.3356,$$
$$\nu_{LT} = 0.3,\ \nu_{TT} = 0.49,\ \alpha_L/\alpha_0 = 0.015,\ \alpha_T/\alpha_0 = 1 \tag{12}$$

- Material Property - II (Isotropic)

$$E_L/E_T = 1,\ G_{LT}/E_T = 0.3846,\ G_{TT}/E_T = 0.3846,$$
$$\nu_{LT} = 0.3,\ \nu_{TT} = 0.3,\ \alpha_L/\alpha_0 = 1,\ \alpha_T/\alpha_0 = 1 \tag{13}$$

- Boundary Condition

$$Clamped: \quad \begin{array}{l} u_0 = v_0 = w_0 = \varphi_y = \varphi_x = 0 \quad \text{on } x = 0, L \\ u_0 = v_0 = w_0 = \varphi_x = \varphi_y = 0 \quad \text{on } y = 0, W \end{array} \tag{14}$$

- 0/90/90/0 Laminate where the 1st and the 3rd layer have Material Property -I and the 2nd and 4th layer have Material Property -II

Results : Hybrid Composites

The critical buckling temperature is normalized as
$\bar{T}_{cr} = 1000 * \alpha_0 * T_{cr}$

Mode	IGA	abaqus
1	0.241	0.245
2	0.310	0.308
3	0.390	0.387
4	0.423	0.425
5	0.485	0.481

Table – critical buckling temperature of a symmetric four-layer [0/90/90/0] laminated plate. Radius/Width=0.15

.

Acknowledgement

Virginia Tech Engineering Mechanics Student Travel Fund for its financial support in making this travel possible

References

1.Jrad, M., De, S. and Kapania, R.K., 2017. Global-Local Aeroelastic Optimization of Internal Structure of Transport Aircraft Wing. In *18th AIAA/ISSMO Multidisciplinary Analysis and Optimization Conference* (p. 4321).

2.De, S., Jrad, M. and Kapania, R.K., 2019. Structural optimization of internal structure of aircraft wings with curvilinear spars and ribs. *Journal of Aircraft*, *56*(2), pp.707-718.

3.Robinson, J.H., Doyle, S., Ogawa, G., Baker, M., De, S., Jrad, M. and Kapania, R.K., 2016. Aeroelastic Optimization of Wing Structure Using Curvilinear Spars and Ribs (SpaRibs). In *17th AIAA/ISSMO Multidisciplinary Analysis and Optimization Conference* (p. 3994).

4.De, S., White, J., Brusuelas, T., Patton, C., Koh, A. and Huang, Q., 2020. Electrochemical behavior of protons and cupric ions in water in salt electrolytes with alkaline metal chloride. *Electrochimica Acta*, *338*, p.135852.

5.De, S., Jrad, M., Locatelli, D., Kapania, R.K. and Baker, M., 2017. SpaRibs geometry parameterization for wings with multiple sections using single design space. In *58th AIAA/ASCE/AHS/ASC Structures, Structural Dynamics, and Materials Conference* (p. 0570).

6.Biswas, S., Saha, D., De, S., Cobb, A.D., Das, S. and Jalaian, B.A., 2021, June. Improving differential evolution through bayesian hyperparameter optimization. In *2021 IEEE Congress on Evolutionary Computation (CEC)* (pp. 832-840). IEEE.

7.De, S., Sides, W.D., Brusuelas, T. and Huang, Q., 2020. Electrodeposition of superconducting rhenium-cobalt alloys from water-in-salt electrolytes. *Journal of Electroanalytical Chemistry*, *860*, p.113889.

8.De, S., Singh, K., Alanbay, B., Kapania, R.K. and Aguero, R., 2018, November. Structural Optimization of Truck Front-Frame Under Multiple Load Cases. In *ASME International Mechanical Engineering Congress and Exposition* (Vol. 52187, p. V013T05A039). American Society of Mechanical Engineers.

9.De, S., Singh, K., Seo, J., Kapania, R., Aguero, R., Ostergaard, E. and Angelini, N., 2019. *Unconventional Truck Chassis Design with Multi-Functional Cross Members* (No. 2019-01-0839). SAE Technical Paper.

10.De, S. and Huang, Q., 2021, May. Mathematical Modeling of Cyclic Voltammogram Curves of Copper Deposition Involving Multiple Additives. In *ECS Meeting Abstracts* (No. 28, p. 977). IOP Publishing.

References

11.De, S., Singh, K., Seo, J., Kapania, R.K., Ostergaard, E., Angelini, N. and Aguero, R., 2021. Lightweight Chassis Design of Hybrid Trucks Considering Multiple Road Conditions and Constraints. *World Electric Vehicle Journal*, *12*(1), p.3.

12.De, S. and Huang, Q., 2020, November. Estimation of Kinetic Parameters of Additives By Semi-Analytical Solution. In *ECS Meeting Abstracts* (No. 17, p. 1483). IOP Publishing.

13.Huang, Q., Sides, W.D., De, S. and Hu, Y., 2019, September. Electrodeposition of Cu, Co and Re from Water in Salt Electrolytes. In *ECS Meeting Abstracts* (No. 46, p. 2116). IOP Publishing.

14.De, S., 2017. *Structural Modeling and Optimization of Aircraft Wings having Curvilinear Spars and Ribs (SpaRibs)* (Doctoral dissertation, Virginia Tech).

15.De, S., Jrad, M., Locatelli, D., Kapania, R.K., Baker, M. and Pak, C.G., 2017. *SpaRibs Geometry Parameterization for Wings with Multiple Sections using Single Design* (No. AFRC-DAA-TN37932).

16.Devarajan, B. and Kapania, R.K., 2020. Thermal buckling of curvilinearly stiffened laminated composite plates with cutouts using isogeometric analysis. *Composite Structures*, *238*, p.111881.

17.Miglani, J., Devarajan, B. and Kapania, R.K., 2018. Thermal buckling analysis of periodically supported composite beams using Isogeometric analysis. In *2018 AIAA/ASCE/AHS/ASC Structures, Structural Dynamics, and Materials Conference* (p. 1224).

18.Li, Q., Devarajan, B., Zhang, X., Burgos, R., Boroyevich, D. and Raj, P., 2016. *Conceptual design and weight optimization of aircraft power systems with high-peak pulsed power loads* (No. 2016-01-1986). SAE Technical Paper.

19.Devarajan, B. and Kapania, R.K., 2022. Analyzing thermal buckling in curvilinearly stiffened composite plates with arbitrary shaped cutouts using isogeometric level set method. *Aerospace Science and Technology*, p.107350.

20.Devarajan, B., 2019. *Thermomechanical and vibration analysis of stiffened unitized structures and threaded fasteners* (Doctoral dissertation, Virginia Tech).

21.Miglani, J., Devarajan, B. and Kapania, R.K., 2021. Isogeometric Thermal Buckling and Sensitivity Analysis of Periodically Supported Laminated Composite Beams. *AIAA Journal*, pp.1-10.

References

22.Devarajan, B., 2021. Vibration Analysis of Timoshenko Beams using Isogeometric Analysis. *arXiv preprint arXiv:2104.12860*.
23.Devarajan, B., 2021. Free Vibration analysis of Curvilinearly Stiffened Composite plates with an arbitrarily shaped cutout using Isogeometric Analysis. *arXiv preprint arXiv:2104.12856*.
24.Devarajan, B., Locatelli, D., Kapania, R.K. and Meritt, R.J., 2016. Thermo-Mechanical Analysis and Design of Threaded Fasteners. In *57th AIAA/ASCE/AHS/ASC Structures, Structural Dynamics, and Materials Conference* (p. 0579).